WORLD CONFERENCE ON TIMBER ENGINEERING 2025
BRISBANE, AUSTRALIA
Advancing Timber for the Future Built Environment

TWO YEARS DYNAMIC MONITORING OF AN EIGHT-STOREY CLT BUILDING

Yue Wang[1], Dag Pasquale Pasca[2], Angelo Aloisio[3], Blaž Kurent[4], Roberto Tomasi[5]

ABSTRACT: This study extensively monitors a Cross-laminated Timber (CLT) building that stands eight stories tall. The monitoring encompasses rooftop acceleration readings coupled with measurements of outside temperature, humidity, and wind speed. In addition, the moisture content (MC) of timber in various parts of the building, especially in the middle and edge walls, is measured. The extraction of modal parameters is automated and is based on the Stochastic Subspace Identification method. The identification of modal parameters is based on the automatic Stochastic Subspace Identification. The core aim of this research is to understand how environmental elements, temperature, wood moisture, and wind speed influence the building's modal characteristics and its response to vibrations. The findings reveal a marked connection between the modal parameters and both temperature and wood moisture levels. Building on this, the researchers use a refined Finite Element (FE) model of the structure to explore the interplay between critical physical factors, particularly moisture and temperature, and their impact on the identified modes. This analysis has led to an empirical formula for predicting the stiffness properties of CLT walls based on wood MC derived from long-term monitoring of a timber building. To the authors' knowledge, it is the first empirical expression relating a mechanical property of timber and MC, indirectly estimated from ambient vibration data.

KEYWORDS: Continuous dynamic monitoring; Cross-Laminated Timber; Environmental effects; FE model updating.

1 – INTRODUCTION

Cross-laminated timber (CLT) is a relatively new engineered wood product. It received its first European technical approval (ETA) in 2006 [1]. The environmental advantages of CLT have contributed to its increasing popularity [2]. These characteristics have made CLT an appealing choice for sustainable construction [3].

Nonetheless, like other engineered wood products, it exhibits significant sensitivity to environmental factors such as temperature and humidity. Additionally, they are highly prone to vibration issues due to the low stiffness-to-mass ratio [4–6]. Over the past thirty years, considerable efforts have been made in long-term monitoring in various construction fields. However, timber has been somewhat overlooked, mainly due to the limited availability of case studies to install permanent monitoring systems. As continuous dynamic monitoring is more systematically applied and CLT has become a leading construction material, the field can be considered mature for exploration.

For timber structures, dynamic data acquisition has been mainly used to obtain an instantaneous understanding of a building's behavior, such as its mode shapes, natural frequency, or response to external excitations like wind and earthquakes [7–11]. More recently, research trends have also shown numerous instances of model updating, employing approaches ranging from deterministic [12,13] to Bayesian [14].

The examples of long-term dynamic monitoring of timber buildings are minimal. Leyder et al. monitored the House of Natural Resources in Switzerland [15] with a post-tensioned timber frame and concrete-timber composite slabs. More recently, Larsson et al. [16] made a significant

[1] Yue Wang, Department of Civil and Architectural Engineering, KTH Royal Institute of technology, Stockholm, Sweden, yue4@kth.se

[2] Dag Pasquale Pasca, Norwegian Institute of Wood Technology, Oslo, Norway, dpa@treteknisk.no

[3] Angelo Aloisio, Civil Constrction-Architecture and Environmental Enginnering Department,Università degli Studi dell'Aquila, L'Aquila, Italy, angelo.aloisio1@univaq.it

[4] Blaž Kurent, Faculty of Civil and Geodetic Engineering, University of Ljubljana, Ljubljana, Slovenia, blaz.kurent@fgg.uni-lj.si

[5] Roberto Tomasi, Norwegian University of Life Sciences, As, Norway, roberto.tomasi@nmbu.no

https://doi.org/10.52202/080513-0070

contribution in this field, with the long-term monitoring of a hybrid timber building, focusing on the dependence of modal parameters on temperature and moisture content.

However, to the authors' knowledge, what remains unexplored is establishing a relationship between the building's modeling parameters and environmental factors, primarily MC and temperature. Additionally, the study focuses on a hybrid, not fully timber structure. Thus, the observed effects cannot be entirely attributed to timber but also its interaction with other construction materials.

Establishing the effect of environmental parameters on the physical properties of wood requires two main contributions: a long-term monitoring system and a finely-tuned finite element (FE) model of the building. This paper provides both elements. After a detailed analysis of the long-term monitoring data, the FE model is used to derive functional relations between the physical parameters and the environmental factors.

This paper presents the long-term continuous dynamic monitoring of an eight-story building that is entirely CLT. This is the first example in the scientific literature where a pure CLT building is monitored and used to assess empirical relationships between the physical properties of wood and its MC and temperature.

2 – CASE STUDY

The studies building is an eight-story student housing structure located in Ås, Norway [12]. The building's overall height is 27 m, excluding a reinforced concrete basement. It features a 23 by 15 m rectangular layout.

The structure is made of CLT panels, including bearing walls and the elevator core. An exterior view of the is presented in Figures 1a and 1b. The structure has large monolithic walls with high length-to-height ratios, assembled using various fasteners such as tie-downs, angle brackets, and screws. Beneath the interior walls, a 10 mm soundproofing layer is installed, which is absent in the external wall-floor joints. The exterior wall is clad with 20 mm thick wooden boards. Indoor walls are generally covered with 25 mm plasterboard, while some are left bare. The floors are layered with an Oriented Stand Board (OSB), a substitute for concrete screed. Most CLT panels have a 5-layer layup from Mayr-Melnhof, except for 90 mm 3-layer panels in a few cases. Wall thickness varies from 100 to 180 mm, and floor slabs from 180 to 220 mm.

In October 2022, the authors installed a permanent monitoring system on the structure's rooftop, as in Figure 1(c). The system consists of three piezoelectric accelerometers and a weather station launched with an anemometer and temperature and humidity sensors, which are summarized in Table 1.

Table 1: Main characteristics of the sensors installed.

Num	Measure	Sensor	Output range	Sensitivity
1	Wind speed	Gill WindMaster ultrasonic anemometer	0-30 m/s	0.16 V/m/s
2	Wind direction		0-360°	0.16 V/°
3	External temperature	Vaisala transmitter HMT333	-40/80°C	0.0625V/°C
4	External humidity		0-100 RH	0.05 V/RH
5	Vibration	Accelerometer (PCB 393B12)	0-1g	10.48 V/g
6	Vibration		0-1g	10.13 V/g
7	Vibration		0-1g	10.13 V/g

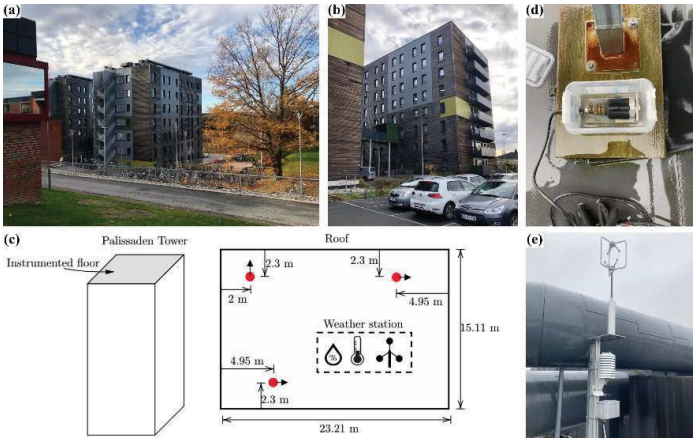

Figure 1. Illustration on the a) single fastener test, b) Case A CPG test, c) Case B CPG test, and d) assembly process of glued-in wooden rods: from drilling, mixing adhesives, pouring adhesive in predrilled holes to inserting rods and curing adhesives.

https://doi.org/10.52202/080513-0070

An independent monitoring system by Omnisense has been implemented within the structure to track the moisture levels in CLT. The research team positioned eleven sensors on internal and external walls across the building's interior. These sensors are catalogued in Table 2, which details their locations.

Table 2: List of the MC sensors installed in the building and their location.

Num	Building position	Direction	CLT Wall position
1	Kitchen	West	Internal
2	Room No. 801	East	Perimeter
3	Room No. 801	South	Perimeter
4	Room No. 809	West	Perimeter
5	Room No. 816	North	Perimeter
6	Staircase No.6	North	Internal
7	Staircase No.6	South	Internal
8	Staircase No.7	North	Internal
9	Staircase No.7	South	Internal
10	Staircase No.8	North	Internal
11	Staircase No.8	South	Internal

Figure 2 presents a typical wireless sensor installed for MC monitoring. In some cases, the installation required plaster removal, as in Figure 2b.

Figure 2. a) A typical sensor monitoring the MC of wood, and (b) plaster removal at some locations.

2.1 MODAL TRACKING

Several methods have emerged to automate operational modal analysis (OMA) within structural health monitoring (SHM) applications. It should be noted that the most suitable method for automated OMA greatly depends on the quality of the data and the specific case study analyzed. It is possible that high-quality data and a case study characterized by stable, well-spaced, and distinct modes and spectral characteristics of the excitation noise that is almost white in the frequency range of interest may render various approaches virtually equivalent.

In this specific study, the authors opted for a semi-automatic approach, given the excellent quality of the data and the stabilization diagrams obtained for various input parameters of the SSI-cov. This approach is characterized by a reduced number of input parameters: the time shift, the minimum and maximum system orders, and the reference frequencies that define the frequency band within which to track the mode. The uncertainty of the modal parameters was estimated using the algorithm proposed by Döhler [68]. Nonetheless, this uncertainty was of an order of magnitude lower than the fourth decimal place and thus considered negligible and not discussed in the current work.

In this application, the authors monitored the evolution of three modes with reference frequencies of 1.88, 2.42, and 2.7 Hz (presented in Figure 4), with tolerances of 0.2 Hz each. Regarding the choice of input parameters, it is worth noting that the SSI-cov algorithm is governed by the following control parameters:

- the number of block rows i (also known as the time shift).
- the length of the data time windows j.
- the model order n.

The efficiency and accuracy of the SSI-cov algorithm depend on the proper selection of i, j, and n. It is noted that these control parameters are not independent of each other. Particularly, a system of order n can be identified as long as the following condition is fulfilled:

$$i \times j \geq n \tag{1}$$

Consequently, the minimum order, $n_{\min}$, can be assumed as a rule of thumb to be twice the number of monitored degrees of freedom l, which equals 3 in the current case study [17].

$$n_{min} = 2 \times l = 2 \times 3 = 6 \tag{2}$$

Theoretically, it is required that $j \rightarrow \infty$. Therefore, the authors did not window the signal and used its entire length (approximately one hour sampled at 200 Hz). The time shift i is still considered a user-defined parameter. Given the importance of this control parameter, after manual tuning, the authors kept it as low as possible to avoid splitting phenomena that occur for too high values of i. Therefore, i was assumed equal to:

$$i = \left\lceil \frac{f_s}{2max\{f_f,1\}} \right\rceil \approx 50 \tag{3}$$

where $\lceil \cdot \rceil$ is the ceiling operation to the nearest integer, f_s the sampling frequency equal to 200 Hz, and f_f the fundamental frequency, assumed equal to 1.8 Hz. The maximum model order $n_{\max}$ comes from Equation 1, assumed equal to $i \times l$. The following soft validation criteria (SC), between consecutive orders, are considered [18–20]:

https://doi.org/10.52202/080513-0070

$$\Delta f = \frac{f_a - f_b}{f_a} \leq 0.01 \quad (4)$$

$$\Delta \xi = \frac{\xi_a - \xi_b}{\xi_a} \leq 0.05 \quad (5)$$

$$1 - MAC(\psi_a, \psi_b) \leq 0.02 \quad (6)$$

Furthermore, the following hard validation criteria (HC), in absolute terms, are considered:

$$\xi \leq 0.1 \quad (7)$$

$$MPC \geq 0.7 \quad (8)$$

$$MPD \leq 0.3 \quad (9)$$

Here the subscripts a, b represent two whichever poles in the stabilization diagram, and MAC is the modal assurance criterion (which represents the measure of the correlation between two modal vectors [18]). Particularly, Eqs. (4)-(6) are denoted as soft criteria (SC) in terms of frequency, damping, and mode shape, respectively, whereas Eqs. (7)-(9) are designated as a hard criterion (HC) on the maximum allowed damping, the minimum allowed value for modal phase collinearity (MPC), and the maximum allowed value for modal phase deviation (MPD) [19,20].

A schematic representation of the procedure is shown as the pseudo-code presented below. This semi-automatic approach allows users to specify the time shift, the model order range, and reference frequencies but then automates evaluating and refining the model within those parameters.

Algorithm 1 Pseudo-code of the algorithm for semi-automatic OMA.

- poles at orders $n = n_{\min}, \ldots, n_{\max}$ from SSI-cov after applying hard and soft criteria.
- j-th reference frequency to track $f_{j,\mathrm{ref},n}$ at the n-th model order.
- relative tolerance, ε

for $n = n_{\min}, \ldots, n_{\max}$ **do**
  for $j = 1, 2, \ldots, k$ **do**
    collect pole(s), if any, that fall within the limits $f_{j,\mathrm{ref},n} \pm \varepsilon$.
  end for
  if the selection of collected poles is equal ($\pm\varepsilon$) to the reference frequencies **then**
    STOP
  end if
end for

Notation: n model order; $n_{\min}$ minimum model order; $n_{\max}$ maximum model order; j the index for the natural frequency; k total number of tracked frequencies; $f_{j,\mathrm{ref},n}$ j-th reference frequency to track at the n-th model order; ε assumed tolerances for the natural frequencies.

Figure 3. A schematic representation of the algorithm for semi-automatic OMA procedure.

3 – RESULTS

3.1 MODAL PARAMETERS AND VIBRATION RESPONSE

Three modes can be intuitively identified in a typical stabilization diagram, as in Figure 4.

The acquisition began in November 2022 and has continued until May 2024. However, there was an interruption in the acquisition from the end of January 2023 to July 2023 due to cable disconnections. The evolution of the peak acceleration as a function of the acquisition time is presented in Figure 5.

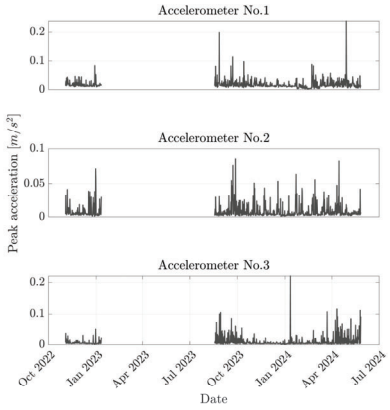

Figure 5. Variation of the peak acceleration of the acquisitions from the three accelerometers as a function of the acquisition date.

The mean, standard deviation, maximum, and minimum values of the peak and root-mean-square acceleration for the three installed accelerometers are presented in Table 3.

Table 3: Mean, standard deviation, maximum, and minimum values of the peak and root-mean-square acceleration for the three accelerometers installed.

Parameters	Num	Mean	Std. Dev.	Max	Min
Peak acceleration [mm/s^2]	1	20.35	16.32	198.68	6.95
	2	9.21	11.62	85.53	1.03
	3	10.14	13.74	105.30	1.22
RMS acceleration [mm/s^2]	1	1.61	1.40	15.40	0.75
	2	1.22	2.01	20.22	0.18
	3	2.00	4.36	40.57	0.19

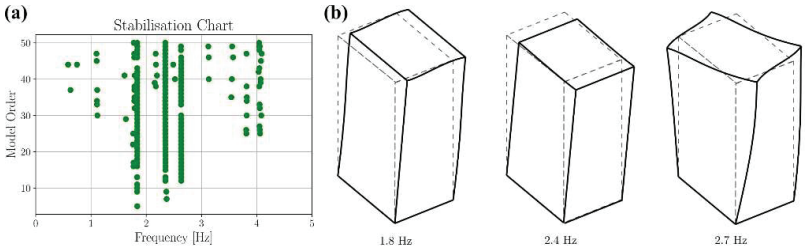

Figure 4. a) Typical stabilization chart from the SSI-cov algorithm, and b) three mode shapes.

https://doi.org/10.52202/080513-0070

The average peak acceleration ranges between 10 and 20 mm/s^2. However, in some cases, the excitation can reach almost 200 mm/s^2. Similarly, the root-mean-square acceleration ranges between 1.5 and 2 mm/s^2, with maxima higher than 40 mm/s^2 in some cases. The response level is not correlated to the wind speed and can be attributed mainly to the human-induced excitation of the occupants.

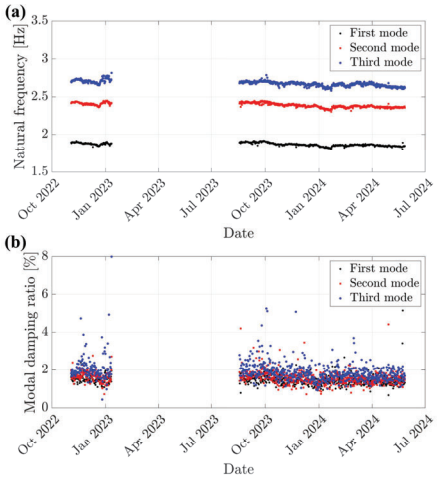

Figure 6. Variation of the (a) natural frequencies and (b) damping ratios, of the first three modes as a function of the acquisition

The variation of the (a) natural frequencies and (b) viscous damping ratios of the first three modes as a function of the acquisition date is presented in Figure 6.

Table 4 presents the mean and standard deviation of the natural frequency and damping ratios of the first three modes.

Table 4: Mean and standard deviation (Std. Dev.) of the natural frequency and damping ratios of the first three modes.

Parameters	First mode		Second mode		Third mode	
	Mean	Std. Dev.	Mean	Std. Dev.	Mean	Std. Dev.
Natural Frequency	1.874	0.022	2.399	0.027	2.688	0.032
Damping ratio	0.015	0.002	0.017	0.003	0.021	0.007

3.2 ENVIRONMENTAL PARAMETERS

The evolution of 1) the external temperature, 2) relative humidity, 3) wind speed, 4) wind direction as a function of the acquisition date are presented in Figures 7c and 7d. Besides, the daily and nightly variations in the MC of CLT walls in different locations are presented in Figures 7e-7h.

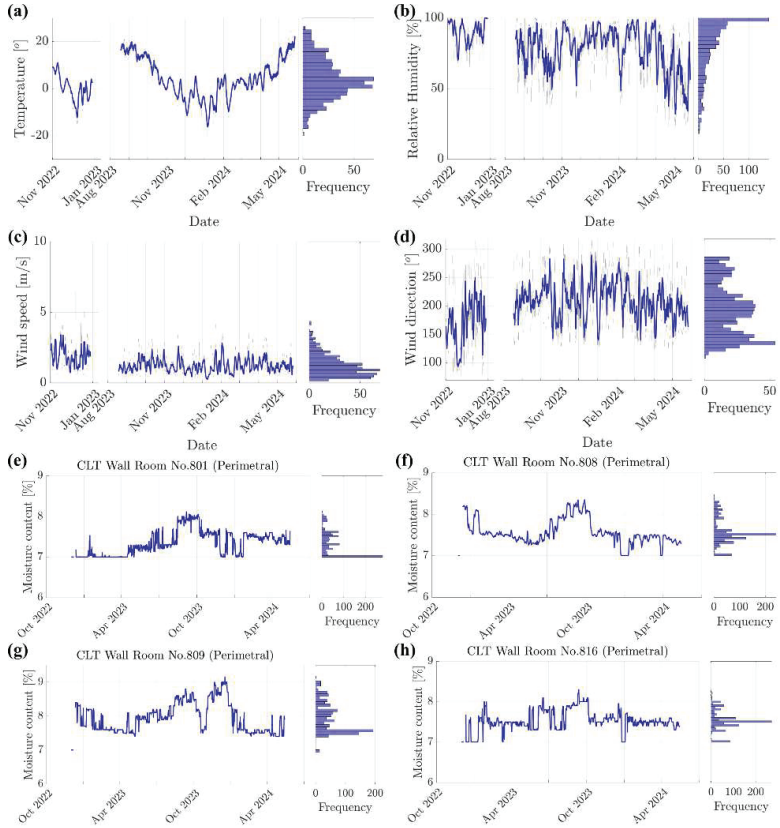

Figure 7.Variation of the (a) external temperature, (b) relative humidity, c) wind speed, and (d) direction as a function of the acquisition date; e-h) Daily and nightly variations in the MC of the perimetral CLT walls. Two data points for each day - one for daytime and one for nighttime.

https://doi.org/10.52202/080513-0070

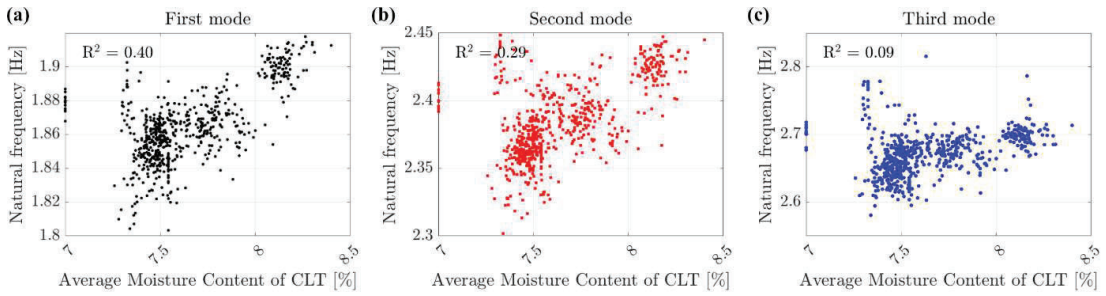

Figure 8. Correlation between natural frequency vs the average MC of the perimeter walls (Room No. 801, 808, 809, and 816).

The MC of the internal walls, with a few exceptions, never exceeds 7%. In contrast, the perimeter walls exhibit evident fluctuations in MC, typically higher than 7%, except for specific measurements taken during fall and winter. Generally, the MC is lower during fall and winter and increases during spring and summer.

The MC of wood tends to be higher during the summer for several reasons. During summer, the increased temperature raises the capacity of the air to retain moisture, which can be absorbed by wood. Furthermore, in winter, indoor heating systems tend to dry out the air inside buildings, thus reducing the MC of wood indoors. In contrast, during summer, the lack of heating and the potential for increased ventilation with outdoor air can lead to higher indoor humidity levels. Additionally, the higher dew points in summer might lead to higher condensation on cooler surfaces of CLT.

3.3 CORRELATION BETWEEN NATURAL FREQUENCIES AND ENVIRONMENTAL MEASUREMENTS

The measured environmental parameters and the natural frequency are presented. As a result, the weather station measurements do not correlate with the modal parameters, except for the external temperature and the MC of the external walls. Due to page limitations, only those parameters depicting correlations are presented here.

The natural frequency data of the first three modes are correlated with the average MC of the perimeter walls (Room No. 801, 808, 809, and 816), and the results are presented in Figure 8.

As a result of observation, the natural frequencies exhibit a positive correlation with MC in the first and second modes, while no significant correlation is observed in the third mode. Interestingly, the data are grouped into three distinct and well-separated clusters for all three modes. This clustering may indicate a shift or discontinuity in the building's dynamics.

To gain further insight into this phenomenon, Fig. 9a shows the relationship between the fundamental frequency and external temperature. In contrast, Fig. 9b depicts the fundamental frequency against the average MC of the perimeter walls. In Fig. 9a, a color gradient from blue to red represents varying MC values, and in Fig. 9b, the color coding is based on temperature values.

While the fundamental frequency exhibits a smooth increase with temperature, its correlation with MC is characterized by distinct clusters. Specifically, the upper-right cluster predominantly includes data from the summer and parts of the fall and spring. In contrast, the bottom-left cluster comprises primarily winter and some fall data. Additionally, a smaller lateral cluster in the central-left part, consisting solely of winter data, corresponds to particularly low MC values.

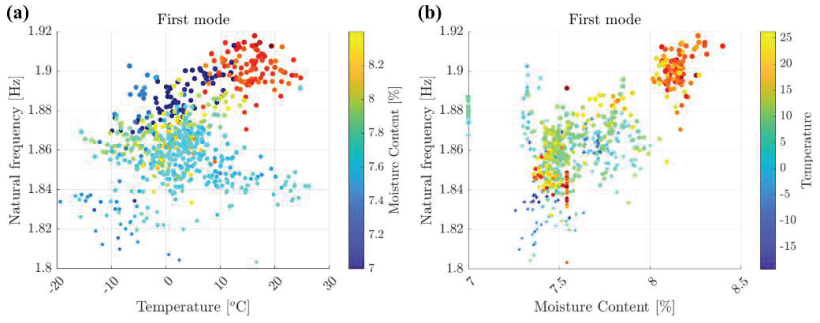

Figure 9. Correlation between natural frequency and (a) the external temperature and (b) average MC.

https://doi.org/10.52202/080513-0070

Besides, the authors observed that the frequencies are not correlated with the fundamental frequency at low temperatures, as shown in Fig. 9b. Consequently, it was explored whether snow depth could be an explanatory parameter using data from a meteorological station in Ås, just a few kilometers away from the studied housing.

The fundamental frequency is plotted against the snow depth in Figure 10, and it is evident that the fundamental frequency decreases almost linearly as the snow depth increases due to the added mass on the building's roof.

3.4 EMPIRICAL REGRESSION MODEL FOR FUNDAMENTAL FREQUENCY PREDICTION

The authors developed two empirical predictive models, given the strong correlations between the fundamental frequency, temperature, MC, and snow height. The first model uses the temperature and MC as input, and the second also includes the snow height. The methods used are linear interaction and machine learning (ML) models. Among the ML approaches evaluated, including regression trees, support vector machine (SVM), and artificial neural network, the SVM with a Gaussian kernel exhibited the best results and was subsequently chosen.

The mathematical formulation of the first linear interaction model is detailed below:

$$f_1 = \beta_0 + \beta_1 \cdot MC + \beta_2 \cdot T + \beta_{12} \cdot MC \cdot T + \varepsilon \quad (10)$$

The second model, including the effect of snow, can be written as:

$$f_1 = \beta_0 + \beta_1 \cdot h_{snow} + \beta_2 \cdot T + \beta_3 \cdot MC + \beta_{12} \cdot h_{snow} \cdot T + \beta_{13} \cdot MC \cdot T + \varepsilon \quad (11)$$

The calibration of the models was conducted using the hold-out method. Data was split into a training set (80%) and a validation set (20%), randomly selected throughout the whole monitoring period.

Table 5 presents the statistical estimates of the linear model parameters obtained using the maximum

Table 5: Statistical estimates of the linear model parameters of the two models. The table lists the parameter estimates along with their standard errors (SE), t-statistics (tStat), and p-values (pValue) for each term in the model.

Parameter	Estimate	SE	tStat	pValue
β_0	1.673	0.028	58.740	0
β_{01}	0.025	0.004	6.522	0.000
β_{02}	-0.019	0.002	-8.400	0.000
β_{12}	0.003	0.000	8.553	0.000
β_0	1.834	0.021	86.171	0.000
β_1	-0.001	0.000	-15.758	0.000
β_2	0.005	0.003	1.661	0.097
β_3	-0.035	0.002	-19.062	0.000
β_{12}	0.000	0.000	5.850	0.000
β_{13}	0.004	0.000	18.996	0.000

The authors also calibrated an SVM regression using a Gaussian kernel [21]. In an SVM regression, the objective is to find a function $f(x)$ that approximates the relationship between the input features x and the response y. This function is based on a set of training data $\{(x_1, y_1), (x_2, y_2), \ldots, (x_n, y_n)\}$, where x_i represents the feature vector of the i-th instance and y_i is its corresponding response. The SVM regression function $f(x)$ is given by:

$$f(x) = \sum_{i=1}^{n} (\alpha_i - \alpha_i^*) K(x, x_i) + b \quad (12)$$

where α_i and α_i^* are the Lagrange multipliers; $K(x, x_i)$ is the Gaussian (RBF) kernel function, and b is the bias term/ The Gaussian kernel $K(x, x_i)$ is defined as:

$$K(x, x_i) = \exp\left(-\frac{\|x - x_i\|^2}{2\sigma^2}\right) \quad (12)$$

Here, σ is the kernel scale parameter, which is set through the 'KernelScale' parameter in the Matlab code. The parameter α_i, α_i^*, and b are determined during the training process, where the model is trained to interpret the data according to the SVM regression criterion. Table 6 presents the SVM parameters.

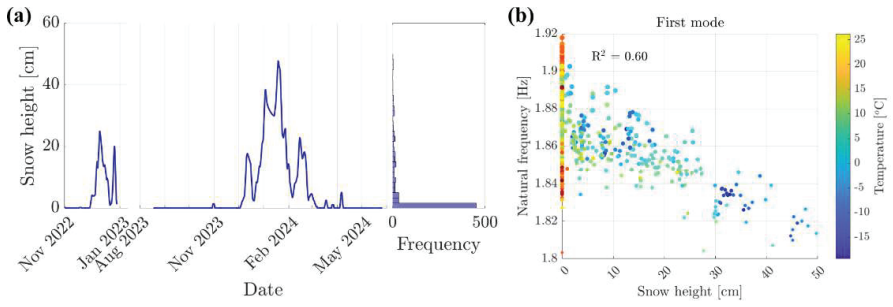

Figure 10. Natural frequency vs (a) external temperature and (b) average MC.

https://doi.org/10.52202/080513-0070

Table 6: SVM Model Parameters.

Parameter	Symbol	Value
Kernel scale	σ	0.350
Mean box constraint	C	0.018
Epsilon	ε	0.0018
Bias	b	1.807

Table 7 compares the performance of the linear and SVM models. The linear interaction model using only temperature and MC as regressors, being the simplest of the two, shows lower performance with an R^2 value close to 0.5, with no indications of overfitting. In contrast, the corresponding SVM model exhibits slightly superior performance, with an R^2 value of 0.5 for the validation set and 0.75 for the training set. It appears that the data quality does not support regressions with an R^2 higher than 0.65 without risking overfitting, a conclusion also reached when employing alternative ML models.

Table 7: Error Metrics for Interaction Linear Model and SVM. The abbreviations are: MAE (Maximum Absolute Error), MSE (Mean Squared Error), RMSE (Root Mean Squared Error), Std. Dev. (Standard Deviation of Error), VAF (Variance Accounted For), and R^2.

Model No.1 - Input: Temperature and MC							
Method	**Set**	**MAE**	**MSE**	**RMSE**	**Std. Dev.**	**VAF**	**R^2**
Interaction linear	Training	0.056	0.0002	0.016	0.016	0.50	0.50
	Validation	0.037	0.0002	0.014	0.014	0.45	0.45
SVM	Training	0.066	0.0001	0.011	0.011	0.75	0.75
	Validation	0.061	0.0002	0.015	0.014	0.53	0.50
Model No.2 - Input: Temperature, MC and snow height							
Method	**Set**	**MAE**	**MSE**	**RMSE**	**Std. Dev.**	**VAF**	**R^2**
Interaction linear	Training	0.047	0.0001	0.011	0.011	0.74	0.74
	Validation	0.049	0.0002	0.013	0.013	0.72	0.72
SVM	Training	0.047	0.0000	0.007	0.007	0.90	0.90
	Validation	0.045	0.0001	0.010	0.010	0.78	0.78

Fig. 11(a)-(b) compares the first empirical model by plotting the measured fundamental frequencies versus the predictions. The SVM model outperforms the linear model, which struggles to fit data at lower natural frequencies. Conversely, the SVM model demonstrates a variance that is almost consistent with the frequency's varying amplitude.

It can also be observed that including snow depth significantly enhances the performance metrics, with R^2 increasing to about 0.7 for the linear model and, on average, 0.8 for the SVM model. This is also evident in Fig. 11(c)-(d). In conclusion, the parameters to consider in model updating include the stiffness properties of CLT, which are affected by MC, temperature, and snow height.

3.4 FEM MODEL OF THE BUILDING AND PHYSICAL PARAMETER CORRELATION

In previous research by the authors [14], an FE model for predicting the modal properties of the building was developed in Ansy, which adopted layered shell elements for modeling CLT panels following the detailed geometry of the building, assuming rigid connections between the panels and elastic support for the foundation.

Monitoring of the building showed a seasonal variation of its modal properties. Since the identified values of the updating parameters depend on the measured natural frequencies, different results may be obtained if the AVT was performed at a different time of the year. To explore this effect, model updating was repeated for each set of identified modal properties of the monitoring.

In this automated model updating, only one parameter was selected - the in-plane shear modulus of the CLT walls, which is based on two reasons. First, with the monitoring, the number of updating parameters needed to be reduced to achieve stable identification. Second, most variation of natural frequencies was assumed to originate from the MC and the additional snow load (can be estimated). MC then remains the most influential variable in monitoring, which is expected to influence the modal properties by changing the in-plane shear stiffness of the CLT panels [16]. Therefore, by using the in-plane shear stiffness as the updating parameter, its seasonal variation as a function of MC can be observed. However, it is worth noting that updating an intricate system may include the effects of more than one parameter.

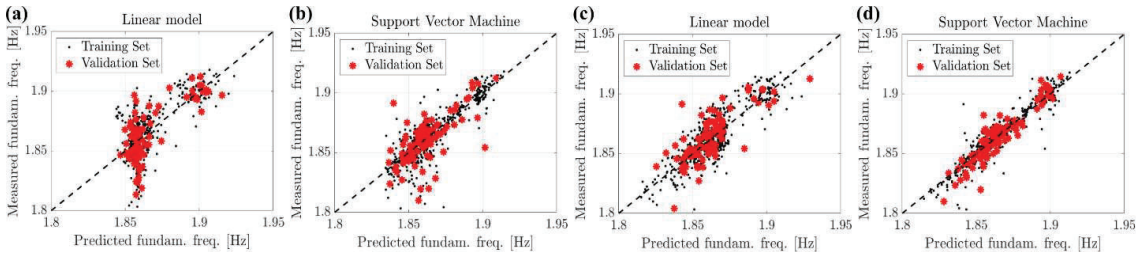

Figure 11. Comparison of empirical models (a),(b) using temperature and MC as regressors, and (c),(d) also including the snow height. (a),(c) show the performance of the linear interaction model, and (b),(d) that of the SVM model. Both models are evaluated in terms of their predicted vs. measured fundamental frequencies.

https://doi.org/10.52202/080513-0070

MC then remains the most influential variable in monitoring, which is expected to influence the modal properties by changing the in-plane shear stiffness of the CLT panels [16]. Therefore, by using the in-plane shear stiffness as the updating parameter, its seasonal variation as a function of MC can be observed. However, the interpretation of the results needs to be taken with caution. Namely, updating an intricate system may include the effects of more than one parameter.

The mathematical formulation of Bayesian inference is not presented in detail due to page limitations. The updated value of the parameter G as a function of the acquisition time is shown in Fig. 12(a), while in Fig. 12(b), G is plotted against the MC with color coding based on the external temperature value. It should be noted that even though parameter G was implemented as an in-plane shear modulus of CLT walls, its updated value does not represent solely a material property. In addition, the updated value also includes the effects of modeling errors that are present due to the inherent nature of the numerical models.

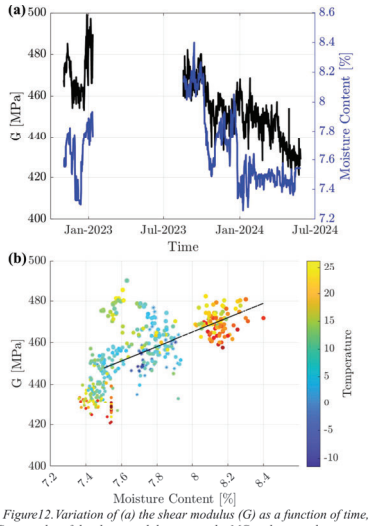

Figure12. Variation of (a) the shear modulus (G) as a function of time, b) Scatter plot of the shear modulus versus the MC and external temperature

First, it is noted that the parameter G exhibits a clear decrease over time and considerable variability across the measurement period. Indeed, as observed, the reduction in G is almost invariably linked to a gradual decline in the MC. The G parameter positively correlates with MC and temperature, as illustrated in Fig. 12(b). The external temperature is indirectly linked to the MC since the decrease in MC during colder months is primarily due to heating systems, which are introduced into the building air with a low water content from outside. Indeed, it is observed that the MC is the independent regressor, as low G values occur not only at low temperatures and low MC but also, as shown in Fig. 12(b) in the lower left, at low MC and higher temperatures. Therefore, the authors opted for correlating the parameter G solely to MC since it is directly and inherently connected to the mechanics of the panel [22,23]. The obtained deterministic linear correlation, excluding points with MC below 7.5%, is:

$$G = 441 + 44.62 \times (\mathrm{MC} - 7.5), where\ MC(\%) \in [7.5,8.8] \quad (13)$$

The $R^2 = 0.63$ indicates a satisfactory correlation despite the large uncertainty that is related to the structural identification, as well as the assumption that MC changes homogeneously over all the CLT panels of the building.

4 – CONCLUSIONS

This paper presents the results of a long-term monitoring project of an eight-story CLT building in Ås, Norway. The long-term monitoring involved measuring the building's vibration response, external environmental parameters (wind direction and speed, external temperature, and external relative humidity), and MC of the selected perimeter and internal CLT walls. The vibration data collected twice daily were processed using the Stochastic Subspace Identification (SSI-cov) method to track the building's modal parameters.

The analysis indicates that the external RH and wind speed did not significantly impact the structure's modal parameters. The relative humidity demonstrates high variability, which precludes a consistent trend in modal parameters, possibly due to a delayed response time. A positive correlation was found between the MC and the fundamental frequency. This relationship, with an R^2 value of approximately 0.4, might be counterintuitive. In colder countries like Norway, heating systems are operational most of the year, leading to a progressive drying of the wood, which peaks at the end of winter. This study suggests that increased temperatures and MC contribute to a stiffer structure, owing to thermal expansion and enhanced friction in timber connections.

Additionally, a strong negative correlation was observed between the fundamental frequency and snow height, which emerged as the second main parameter for explaining the variability in the modal data. The analysis of experimental data indicates that temperature, MC, and snow height significantly influence modal parameters. The first two factors are tied to the mechanical properties of CLT, while the third is external.

Besides, the authors have implemented a continuous Bayesian FE model updating strategy, focusing on updating the in-plane shear modulus of the CLT walls. A

https://doi.org/10.52202/080513-0070

relationship between the shear modulus and MC based on the vibration data has been achieved, achieving an R^2 value of 0.63. In contrast to the existing literature, which focuses on the empirical relationships between modal and environmental parameters, this effort marks the first attempt to derive an empirical relationship for the mechanical properties of CLT from long-term vibration-based monitoring.

5 – REFERENCES

[1] R. Brandner, Production and Technology of Cross Laminated Timber (CLT): A state-of-the-art Report, in: Focus Solid Timber Solut. Conf. Cross Laminated Timber, University of Bath, Bath, UK, 2013: pp. 3–36.

[2] M. Dorn, Investigations on the Serviceability Limit State of Dowel-Type Timber Connections, Technische Universität Wien, 2012.

[3] M. Bazli, M. Heitzmann, H. Ashrafi, Long-span timber flooring systems: A systematic review from structural performance and design considerations to constructability and sustainability aspects, J. Build. Eng. 48 (2022) 103981.

[4] J. Weckendorf, E. Ussher, I. Smith, Dynamic response of CLT plate systems in the context of timber and hybrid construction, Compos. Struct. 157 (2016) 412–423.

[5] E. Ussher, K. Arjomandi, I. Smith, Status of vibration serviceability design methods for lightweight timber floors, J. Build. Eng. 50 (2022) 104111.

[6] A. Aloisio, D.P. Pasca, Y. De Santis, T. Hillberger, P.F. Giordano, M.M. Rosso, R. Tomasi, M.P. Limongelli, C. Bedon, Vibration issues in timber structures: A state-of-the-art review, J. Build. Eng. 76 (2023) 107098.

[7] T. Reynolds, R. Harris, W.-S. Chang, Ambient Vibration Testing and Modal Analysis of Multi-Storey Cross-Laminated Timber Buildings, in: Timber Res. Dev. Agency Res. Summ., 2014.

[8] I. Mugabo, A.R. Barbosa, M. Riggio, J. Batti, Ambient vibration measurement data of a four-story mass timber building, Front. Built Environ. 5 (2019) 67.

[9] Y. Miyazu, C. Loss, Lateral vibration data of an 18-story timber-concrete hybrid building obtained by on-site vibration tests, Data Br. 50 (2023) 109501.

[10] W.K. Ao, A. Pavic, B. Kurent, F. Perez, Novel FRF-based fast modal testing of multi-storey CLT building in operation using wirelessly synchronised data loggers, J. Sound Vib. 548 (2023) 117551.

[11] B. Kurent, B. Brank, W.K. Ao, Model updating of seven-storey cross-laminated timber building designed on frequency-response-functions-based modal testing, Struct. Infrastruct. Eng. 19 (2023) 178–196.

[12] A. Aloisio, D. Pasca, R. Tomasi, M. Fragiacomo, Dynamic identification and model updating of an eight-storey CLT building, Eng. Struct. 213 (2020) 110593.

[13] B. Kurent, W.K. Ao, A. Pavic, F. Pérez, B. Brank, Modal testing and finite element model updating of full-scale hybrid timber-concrete building, Eng. Struct. 289 (2023) 116250.

[14] B. Kurent, N. Friedman, W.K. Ao, B. Brank, Bayesian updating of tall timber building model using modal data, Eng. Struct. 266 (2022) 114570.

[15] C. Leyder, E. Chatzi, A. Frangi, Vibration-based model updating of a timber frame structure, Procedia Eng. 199 (2017) 2132–2139.

[16] C. Larsson, O. Abdeljaber, Å. Bolmsvik, M. Dorn, Long-term analysis of the environmental effects on the global dynamic properties of a hybrid timber-concrete building, Eng. Struct. 268 (2022) 114726.

[17] E.N. Chatzi, M.D. Spiridonakos, A.W. Smyth, Implementation of parametric methods for the treatment of uncertainties in online identification, Identif. Methods Struct. Heal. Monit. (2016) 51–87.

[18] C. Rainieri, G. Fabbrocino, Operational modal analysis of civil engineering structures, Springer, New York 142 (2014) 143.

[19] G. Zini, M. Betti, G. Bartoli, A quality-based automated procedure for operational modal analysis, Mech. Syst. Signal Process. 164 (2022) 108173.

[20] E. Reynders, J. Houbrechts, G. De Roeck, Fully automated (operational) modal analysis, Mech. Syst. Signal Process. 29 (2012) 228–250.

[21] V.N. Vapnik, An overview of statistical learning theory, IEEE Trans. Neural Networks 10 (1999) 988–999.

[22] F.P. Kollman, Principles of wood sciences and technology, I. Solid Wood (1968) 257–274.

[23] J. Bodig, B.A. Jayne, Mechanics of wood and wood composites, (1982).